



Universiteit
Leiden
The Netherlands

Chemical tools to monitor and control human proteasome activities

Bruin, G. de

Citation

Bruin, G. de. (2016, June 1). *Chemical tools to monitor and control human proteasome activities*. Retrieved from <https://hdl.handle.net/1887/39834>

Version: Not Applicable (or Unknown)

License: [Licence agreement concerning inclusion of doctoral thesis in the Institutional Repository of the University of Leiden](#)

Downloaded from: <https://hdl.handle.net/1887/39834>

Note: To cite this publication please use the final published version (if applicable).

Cover Page



Universiteit Leiden



The handle <http://hdl.handle.net/1887/39834> holds various files of this Leiden University dissertation.

Author: Bruin, G. de

Title: Chemical tools to monitor and control human proteasome activities

Issue Date: 2016-06-01

CHAPTER 10

A native-PAGE FRET assay that reports on mammalian proteasome core particle composition

Introduction

26S proteasomes are responsible for the degradation of the majority of cytoplasmic and nuclear proteins in eukaryotic cells.¹ Proteins destined for degradation are tagged with poly-ubiquitin chains for recognition by 19S (PA700) caps. Subsequently and in an ATP-dependent process, proteasome substrates are unfolded and funnelled through the α -rings to the inner side of 20S proteasome core particles (CP), where they are degraded. CPs are 28-mer multi-protein complexes consisting of four heptameric rings: two outer α -rings onto which 19S caps can dock and two inner β -rings in which the catalytic subunits reside. Each β -ring of the constitutive proteasome (cCP, Figure 1), constitutively expressed in all eukaryotic cells, contains three different active subunits: β 1c (caspase-like, cleaving preferentially after acidic residues), β 2c (trypsin-like, cleaving preferentially after basic residues) and β 5c (chymotrypsin-like, cleaving preferentially after hydrophobic residues). Proteasomes produce oligopeptides varying in length between 3-12 residues.² These are further processed by aminopeptidases and in part escape to the ER lumen, where they bind to major histocompatibility complex class I (MHC-I) heterodimers for antigen presentation. Another type of proteasomes, immunoproteasomes (iCP, Figure 1), are constitutively expressed in bone marrow derived cells and can be induced in other tissues by the inflammatory cytokines, interferon- γ (IFN- γ) and tumour necrosis factor- α (TNF- α).³ iCPs generate peptide pools containing a comparatively (with respect to cCP-produced oligopeptide pools) higher number of peptides prone to bind to MHC-I complexes. This change is mainly caused by the substrate specificity of β 1i, which appears chymotrypsin-like in nature, as compared to the caspase-like nature of β 1c. The cleavage specificity of β 2i and β 5i resembles their cCP counterparts, β 2c and β 5c. Besides 19S caps, CPs can also interact with other proteasome activators including PA28 (or 11S) and PA200.⁴ In addition, hybrid CPs can be simultaneously

bound to 19S, 11S or PA200 to form hybrid proteasomes.⁵ 11S containing proteasome complexes degrade proteins in an ATP-independent manner, are more active and cause generation of peptides that are not suitable for binding to MHC-I. The exact role of 11S caps in the immune system remains elusive.⁴

Constitutive proteasome assembly

In the formation of mammalian constitutive proteasomes, α -rings are assembled first and serve as a scaffold onto which the β -subunits dock.^{6, 7} In this manner $\alpha_7\beta_7$ complexes are formed. These dimerise to form $\alpha_7\beta_7\beta_7\alpha_7$ preholoproteasome cCPs, which, after a number of proteolytic steps, yield fully active cCPs. Correct α -ring formation is mediated by two proteasome assembling chaperones (PACs), heterodimeric protein complexes termed PAC1-PAC2⁸ and PAC3-PAC4.⁹ PAC1-PAC2 binds α_5 and α_7 simultaneously and remains associated until cCP formation nears completion (Figure 1B).⁸ PAC3-PAC4 binds to α_5 and the resulting complex serves as scaffold from which an α -ring emerges.^{7, 9} A fully assembled α -ring next binds to the maturation protein (POMP, or UMP1)¹⁰. Subsequently, β_2 docks onto the α -ring¹¹, followed by β_3 and release of PAC3-PAC4. The resulting assembly is termed a 15S complex and consists of a single α -ring binding to PAC1-PAC2, β_2 and β_3 .¹² Next and in this order β_4 , β_5 , β_6 , β_1 and β_7 are incorporated. The β_7 C-terminal tail then intercalates between β_1 and β_2 of another $\alpha_7\beta_7$ particle, thereby triggering dimerization and formation of a preholoproteasome cCP.¹² Most β -subunits are expressed with N-terminal and/or C-terminal extensions, which function as intramolecular chaperones and are cleaved during the assembly process. The β_{1c} , β_{2c} and β_{5c} subunits are translated with N-terminal propeptides that remain intact until the final stages of proteasome formation.¹³ Autocatalytic removal of both N-terminal and C-terminal propeptides followed by degradation of the chaperones, POMP and PAC1-PAC2 yields functional 20S proteasome cCPs, with the $\beta_{1c}/\beta_{2c}/\beta_{5c}$ catalytic, N-terminal threonine residues revealed at this final stage.^{8, 14}

Immunoproteasome assembly

The assembly of iCP particles is similar to that of cCPs, however with some striking differences. Whereas β_{1c} is incorporated as the second-to-last β -subunit, β_{1i} enters the assembly pathway much earlier and forms an intermediate complex with β_{2i} , β_3 and β_4 (Figure 1C).^{15, 16} β_{5i} has a higher affinity for POMP than β_{5c} and is therefore incorporated preferentially over β_{5c} when both particles are present.¹⁵ In addition, β_{5i} is required for maturation of β_{1i} and β_{2i} .¹⁷ These interdependencies guide a preferential formation of homogenous 20S core particles (iCPs) that contain β_{1i} , β_{2i} and β_{5i} , even though constitutive proteasome catalytic activities (β_{1c} , β_{2c} , β_{5c}) are always present during iCP formation.

Mixed proteasomes

iCPs and cCPs are however not formed exclusively in tissue expressing both active β -subunit sets ($\beta 1c/\beta 2c/\beta 5c$ and $\beta 1i/\beta 2i/\beta 5i$), and mixed proteasomes (mCPs) containing cCP and iCP catalytic subunits can be formed (Figure 1A). Since $\beta 1i$ and $\beta 2i$ both rely on $\beta 5i$ for removal of their N-terminal propeptide, $\beta 5i$ is always present in mCPs in at least one of the two β -rings.

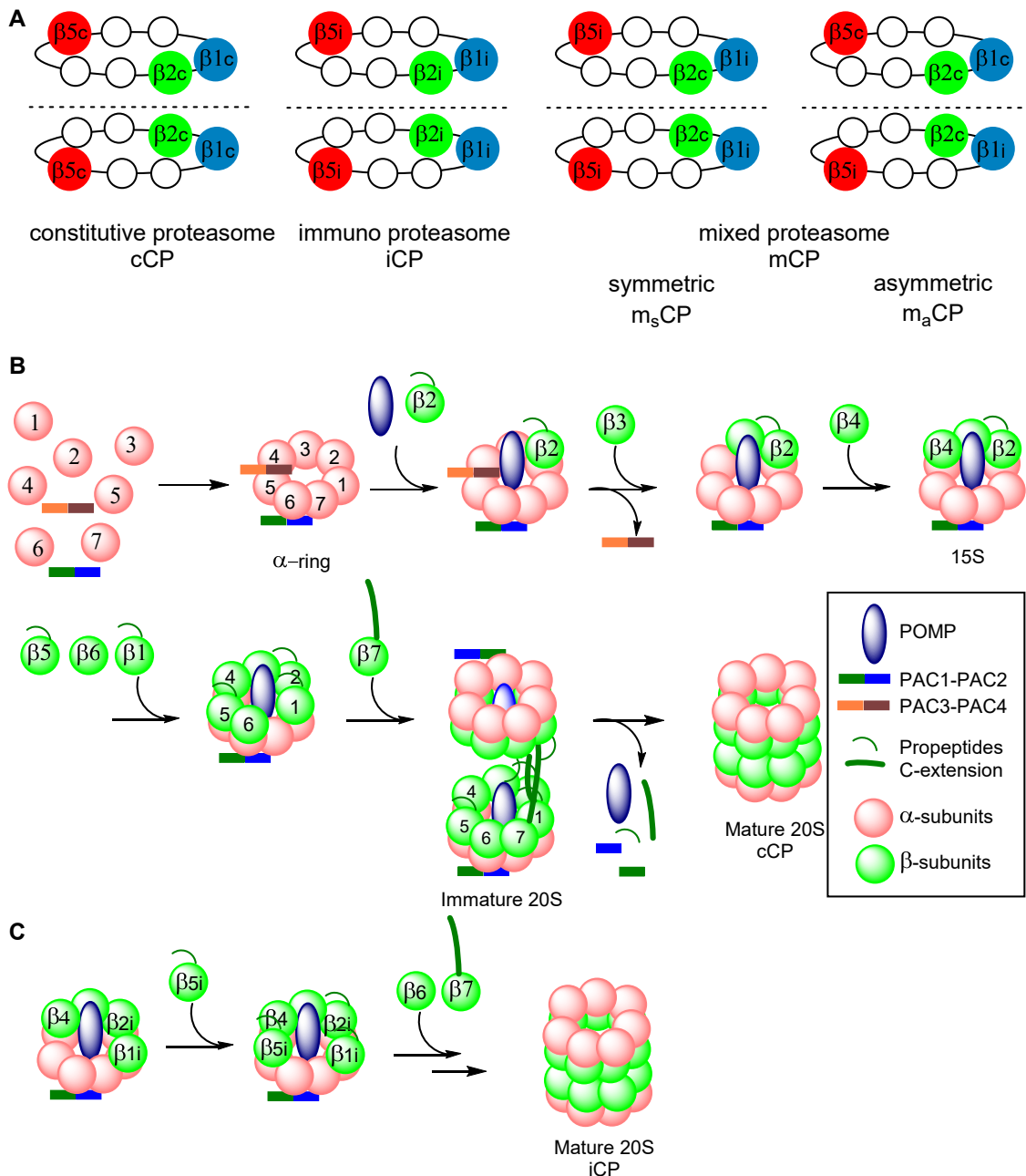


Figure 1. Proteasome subtypes and assembly. A) Schematic representations of cCP, iCP and some m_s CPs and m_a CPs. B) Assembly pathway of cCPs. C) Assembly of the iCP.

Subtype	$\beta 1$	$\beta 2$	$\beta 5$	$\beta 1$	$\beta 2$	$\beta 5$	Subtype	$\beta 1$	$\beta 2$	$\beta 5$	$\beta 1$	$\beta 2$	$\beta 5$
cCP							m_aCP_4						
iCP							m_aCP_5						
m_sCP_1							m_aCP_6						
m_sCP_2							m_aCP_7						
m_sCP_3							m_aCP_8						
m_aCP_1							m_aCP_9						
m_aCP_2							m_aCP_{10}						
m_aCP_3													

Table 1. Theoretical possible proteasome subtypes. With the prerequisite that $\beta 5i$ is always present in a β -ring when $\beta 1i$ and/or $\beta 2i$ are incorporated, 15 subtypes are possible. **Grey:** constitutive proteasome subunit. **White:** immunoproteasome subunit.

Incorporation of $\beta 2i$ and $\beta 1i$ are mutually dependent to some extent, although $\beta 1i$ can be incorporated with $\beta 2c$ and $\beta 2i$ with $\beta 1c$.¹⁷⁻¹⁹ During proteasome assembly, two half proteasomes ($\alpha_7\beta_7$) are joined to form, upon autocatalytic removal of the β -subunit propeptides, mature 20S particles ($\alpha_7\beta_7\beta_7\alpha_7$). In this process, β -rings may have the same β -subunit composition, leading to cCPs, iCPs or symmetric, mixed CPs (m_sCPs). Asymmetric, mixed proteasomes (m_aCPs) are formed when two differently composed $\alpha_7\beta_7$ particles are joined.^{20, 21} Mathematically, different CP particles are possible, however, $\beta 1i$ and $\beta 2i$ can only be incorporated together with $\beta 5i$. Taking this restriction in account, five different β -rings are possible, and thus 15 different proteasome types may exist simultaneously in cells expressing all cCP and iCP subunits (Table 1). Of the 15 possible combinations, mCPs containing either $\beta 5i$ - $\beta 1c$ - $\beta 2c$ or $\beta 5i$ - $\beta 1i$ - $\beta 2c$ β -rings are encountered most often and have been identified in human liver, colon, small intestine and kidney tissues.²² mCPs produce peptide pools distinct from both those produced by cCPs and iCPs, thus adding to the diversity of MHC-I ligands and thereby to a broad CD8⁺ T-cell repertoire. Tumour-specific antigenic peptides^{22, 23} as well as virally encoded antigenic peptides²⁴ have been identified that appear to be produced uniquely by mCPs. A rapid and accurate assay to detect mixed proteasomes and that would report on the nature of their composition would be of considerable use to get insight in the contribution of these in protein turnover and MHC-I antigenic peptide pool production.

Analysis of proteasome composition

Current methods to identify proteasome CP composition are based on either chromatographic separation of proteasome subtypes,^{21, 25} isoelectric focussing electrophoresis,²⁶ or antibody mediated depletion of a β -subunit,²² followed by determination of CP composition by either immunostaining, substrate hydrolysis assays or mass spectrometry analysis of purified proteasomes.²⁷ This chapter describes a native-PAGE

Fluorescence Resonance Energy Transfer (FRET) assay that reports on proteasome CP composition of crude cell lysates. For this purpose proteasome-subunit selective irreversible inhibitors were equipped with suitable fluorophores to yield a panel of activity-based probes (ABPs) for FRET mediated detection of proteasome compositions. FRET is a physical process in which energy is transferred from a donor fluorophore to an acceptor fluorophore via dipole-dipole coupling. This non-radiative energy transfer depends on whether the fluorophores are in close proximity ($>100 \text{ \AA}$); whether there is substantial overlap between the donor emission and acceptor excitation spectra and whether the fluorophores are properly oriented (the dipoles of the fluorophores should be approximately parallel).²⁸ FRET has been widely used to study protein-protein interactions and conformational changes,²⁹ but its potential to determine the composition of protein complexes has not been fully exploited.³⁰ The distances between all active site threonine residues fall well within the FRET range ($<100 \text{ \AA}$)³¹ (Figure 2). This chapter describes the development and use of activity-based probes (ABPs) that target either human $\beta 1c/\beta 1i$, $\beta 2c/\beta 2i$ or $\beta 5c/\beta 5i$ and that are equipped with suitable FRET donor or acceptor fluorophores. With these, in combination with simultaneous selective inhibition of multiple sites, eight distinct CP subunit-combinations, originating from cCPs, iCPs and m_s CPs, were detected using native-PAGE FRET. In addition, ABPs targeting either $\beta 1c$, $\beta 1i$, $\beta 5c$ or $\beta 5i$ were used to discern asymmetric, mixed proteasomes (m_a CPs).

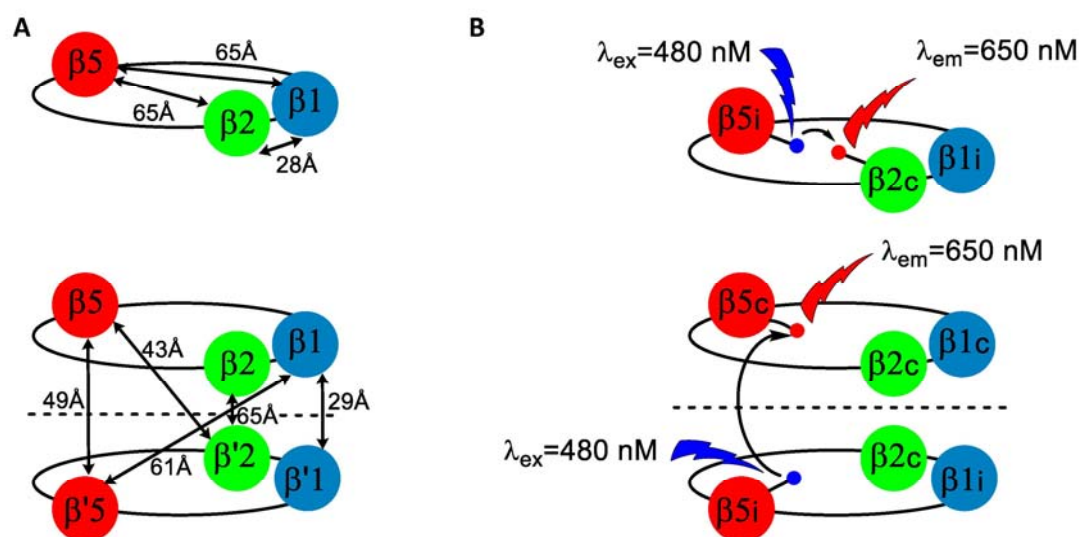


Figure 2. A) Distances between active site Thr residues. B) Examples of intra- (top) and inter- β -ring FRET (bottom) between a donor ABP (small blue sphere, BODIPY-FL fluorophore) and an acceptor ABP (small red sphere, Cy5 fluorophore).

Results

Development of FRET donor and acceptor ABPs

Native-PAGE separation of proteasomes has provided important insights in proteasomal composition, assembly and binding characteristics.³² On native gel, proteasome complexes separate in three bands, corresponding to doubly capped 30S proteasomes, singly capped 26S-proteasomes and 20S proteasome CPs. These complexes are revealed by either Western blotting or in-gel fluorogenic substrate assays.³² Proteasomes containing 11S or PA200 caps have not been investigated using native-PAGE to date. It was reasoned that, in analogy to SDS-PAGE, it should be possible to visualize intact proteasome complexes on native-PAGE using ABPs. Indeed (Figure 3, lane 1-3), clear labelling of both 26S proteasomes and 20S proteasomes was observed in crude cell lysate using either Cy5-NC001 (β 1-selective), BODIPY(FL)-LU112 (β 2-selective) or BODIPY(TMR)-NC005 (β 5-selective; see chapter 3 for the development of these probes). In the first instance it was investigated whether FRET signals emerge from proteasomes exposed to combinations of these probes and next resolved by native-PAGE. For this purpose, lysates were treated with each of the three combinations of two probes simultaneously. Clear FRET signals could be observed for each combination (Figure 3, lane 4-6, Cy2-Cy3, Cy3-Cy5 and Cy2-Cy5 channels) as well as quenching of FRET donor ABPs (Figure 3, Cy2-Cy3 channels, lane 4-6 compared to lane 2-3).

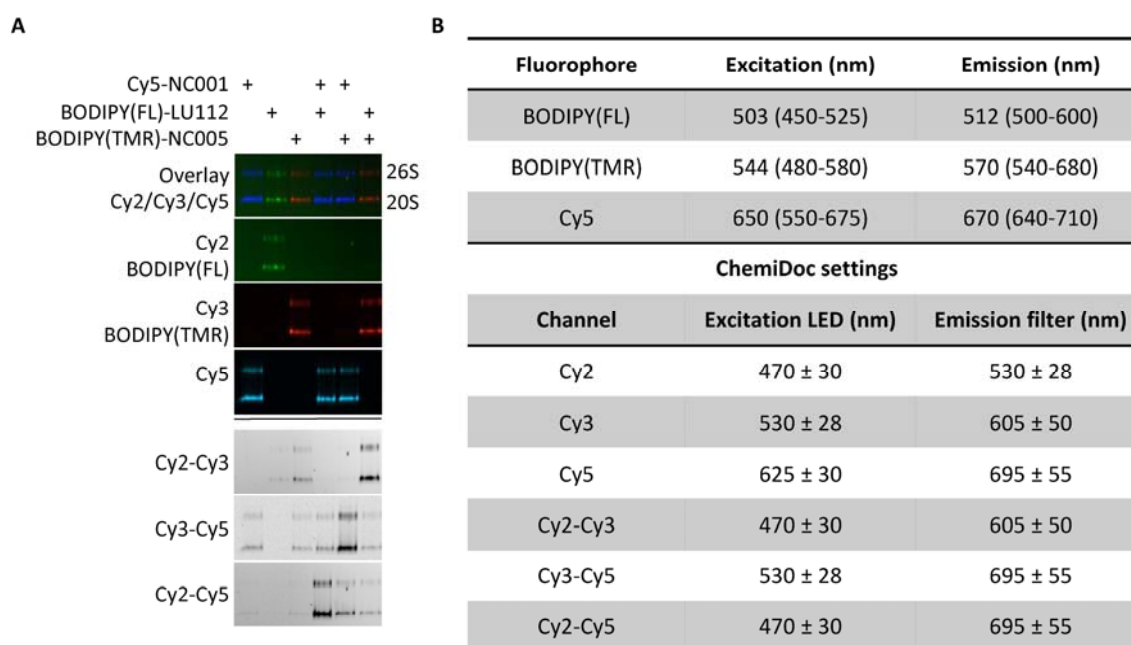


Figure 3. Selection of a suitable FRET donor/acceptor pair. A) Native-PAGE analysis of Raji lysate labelled with individual probes and with three different donor/acceptor pairs. B) Excitation/emission of fluorophores and settings on the ChemiDoc gel imager.

However, due to the spectral overlap with both Cy2 excitation and Cy5 emission, the use of BODIPY(TMR) as either FRET donor or acceptor proved suboptimal (Figure 3, lane 3, Cy2-Cy3 and Cy3-Cy5 channels, notice the background signals). In the Cy2-Cy5 channel, hardly any background signal was observed in the samples treated with BODIPY(FL)- or Cy5-modified probes (Figure 3, lane 1 and 2, Cy2-Cy5). As well, FRET efficiency between these fluorophores appeared close to 100%, indicating near complete quenching of BODIPY(FL) fluorescence. Given these results, it was decided to develop BODIPY(FL) and Cy5 ABPs for each subunit-pair ($\beta1c/\beta1i$, $\beta2c/\beta2i$ and $\beta5c/\beta5i$). The structures of all ABPs used in this study are shown in Figure 4. BODIPY(FL)-NC001³³ **2** and BODIPY(FL)-LU112³⁴ **4** have been described previously, whereas Cy5-LU112 **3** was readily synthesised following established procedures (see the experimental section). Cy5-LU015 **5** and BODIPY(FL)-LU015 **6** were used to selectively label $\beta5c/\beta5i$ (see chapter 6). Furthermore, in order to study m_a CPs, ABPs selective for a single catalytic subunit, namely BODIPY(FL)-LU001c **7** ($\beta1c$ -selective, see chapter 8), Cy5-LU001i **8** ($\beta1i$ -selective, see chapter 6), BODIPY(FL)-LU015c **9** ($\beta5c$ -selective, see chapter 7) and Cy5-LU035i **10** ($\beta5i$ -selective, see chapter 6), were developed. The selectivity window of ABPs **1-10** was assessed in Raji- and HEK cell lysates (ABP **1-6**) and the required concentrations for complete labelling of the respective subunits are indicated in Table 2 (see supplemental Figure 1 for labelling profiles). $\beta2$ -selective probes **3** and **4** as well as $\beta1$ -selective probe **2** partially label both $\beta5$ subunits at concentrations required for full labelling. To avoid this to happen, the $\beta5$ subunits are to be blocked previous to treatment with **2**, **3** or **4** and this can be accomplished by pre-treatment with either a $\beta5$ -selective inhibitor or by $\beta5$ probes **5** or **6** (neither of which are cross-reactive). $\beta5c$ selective probe BDP-LU015c **9** partially labels both $\beta2$ subunits, which however can be prevented by pre-treatment with the $\beta2$ -selective inhibitor LU102 (**12**) (see chapter 7).

Evaluation of ABPs 1-6 as native-PAGE FRET proteasome probes

From the pool of ABPs **1-6**, six FRET donor/acceptor pairs can be assembled. All these pairs were evaluated in Raji and HEK-293 lysates on their behaviour as FRET couples in a native-PAGE fluorescence readout setting. In the first step, both $\beta5$ subunits were either inhibited with NC-005 **13** (in case FRET signals emerging from ABP labelling of $\beta1$ and $\beta2$ were sought for) or labelled with ABPs **6** or **7** ($\beta1$ - $\beta5$ or $\beta2$ - $\beta5$ labelling) for 1 hour. Subsequently, $\beta1$ and/or $\beta2$ targeting probes **1**, **2**, **3** and/or **4** were added and the samples were again incubated for 1 hour. One half of each sample was resolved by native-PAGE and the other half by SDS-PAGE. Clear FRET signals and near complete quenching of FRET donor ABPs were observed for each FRET pair (Figure 5A). Following quantification of the fluorescence bands of the acceptor ABPs (Cy2 channel), the FRET efficiencies (E) were calculated, and high FRET efficiencies for each FRET pair (E > 0.8, Figure 5B) were revealed.

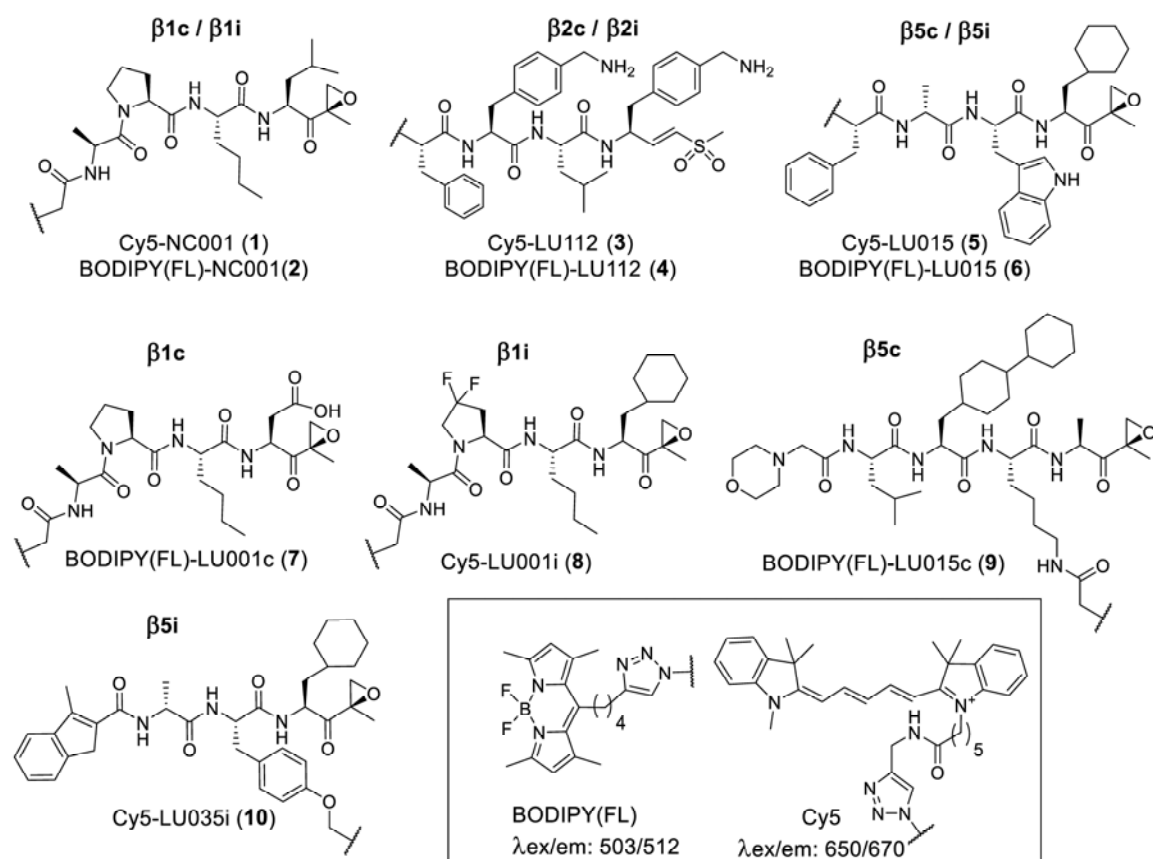
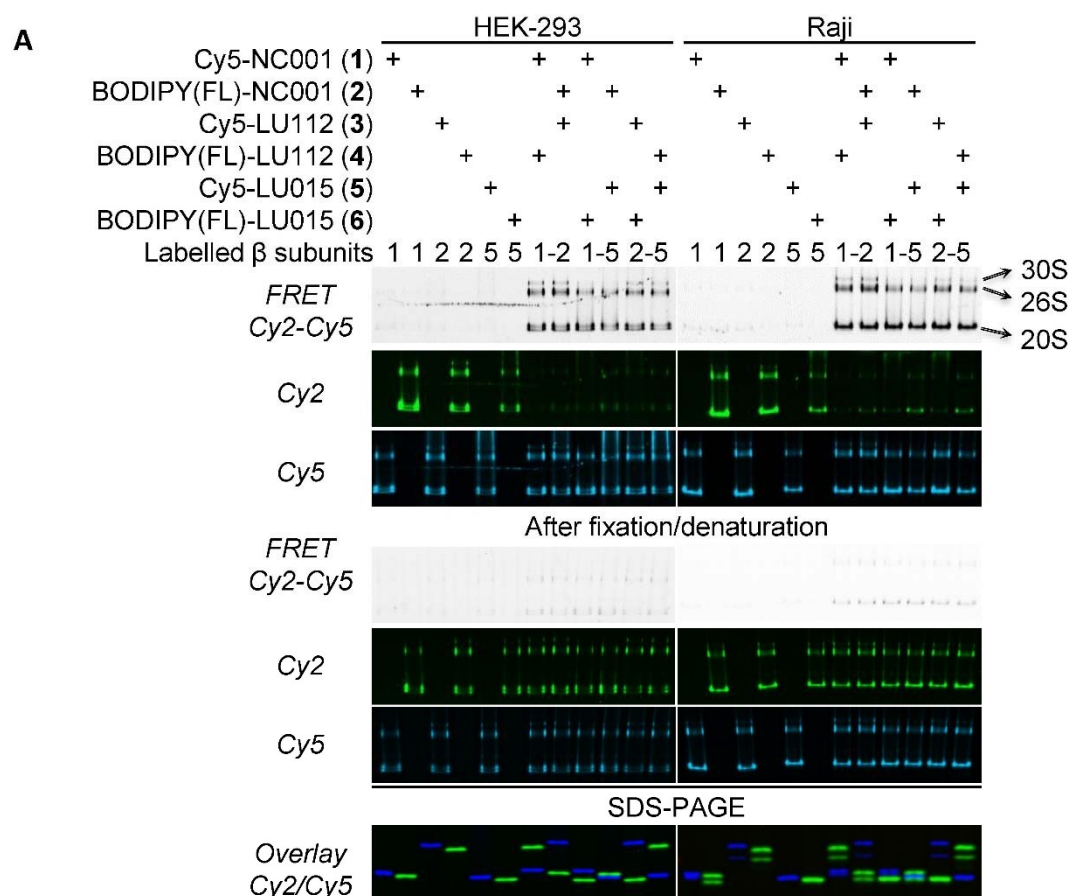


Figure 4. Structures of FRET donor (BODIPY(FL)) and acceptor (Cy5) activity-based probes used in this study.

[ABP] (μM)	Subunit	Raji	HEK (HeLa)	[inhibitor] (μM)	Subunit	Raji (HeLa)		
1	Cy5-NC001	β_{1c}/β_{1i}	0.3	0.1	11	NC001	β_{1c}/β_{1i}	2.5
2	BODIPY(FL)-NC001	β_{1c}/β_{1i}	1.0	1.0	12	LU102	β_{2c}/β_{2i}	0.3
3	Cy5-LU112	β_{2c}/β_{2i}	0.03	0.1	13	NC005	β_{5c}/β_{5i}	2.5
4	BODIPY(FL)-LU112	β_{2c}/β_{2i}	0.1	0.1	14	LU001c	β_{1c}	3.0 (10)
5	Cy5-LU015	β_{5c}/β_{5i}	0.3	1.0 (0.3)	15	LU001i	β_{1i}	1.0
6	BODIPY(FL)-LU015	β_{5c}/β_{5i}	0.3	1.0* (0.3)	16	LU002i	β_{2i}	3.0
7	BODIPY-LU001c	β_{1c}	0.1	n.d. (0.1)	17	LU005c	β_{5c}	1.0 (3)
8	Cy5-LU001i	β_{1i}	0.1	n.d. (0.1)	18	LU035i	β_{5i}	0.3
9	BODIPY-LU015c	β_{5c}	0.3	n.d. (0.3)				
10	Cy5-LU035i	β_{5i}	0.1	n.d. (0.1)				

Table 2. Concentrations for full labelling by ABPs or full inhibition by inhibitors for the target subunit(s). n.d.: not determined. * 80% inhibition after 2 h.

Swapping the FRET donor (BODIPY-FL) and acceptor (Cy5) on the subunit-selective ABPs did not result in significant differences in FRET efficiency. In order to verify whether true intra-proteasomal FRET signals are observed, the native-PAGE slab was transferred to a fixing solution (5:4:1 H₂O/MeOH/AcOH) and heated in a microwave oven. This process results in denaturation of the proteins, and separation of the fluorophores. Indeed, after fixation, FRET signals have disappeared almost entirely (Figure 5A), with concomitant return of fluorescence of the donor ABPs.



B

FRET Efficiency $E=1-(F_{DA}/F_D)$				
Donor	Acceptor	Subunits	E (HEK)	E (Raji)
BODIPY(FL)-LU112 (4)	Cy5-NC001 (1)	β_2 - β_1	0.96	0.96
BODIPY(FL)-NC001 (2)	Cy5-LU112 (3)	β_1 - β_2	0.93	0.93
BODIPY(FL)-LU015 (6)	Cy5-NC001 (1)	β_5 - β_1	0.82	0.85
BODIPY(FL)-NC001 (2)	Cy5-LU015 (5)	β_1 - β_5	0.87	0.86
BODIPY(FL)-LU015 (6)	Cy5-LU112 (3)	β_5 - β_2	0.81	0.85
BODIPY(FL)-LU112 (4)	Cy5-LU015 (5)	β_2 - β_5	0.87	0.81

Figure 5. Evaluation of six FRET donor/acceptor pairs in HEK-293 and Raji lysates. A. Native-PAGE and SDS-PAGE analysis. Gels were imaged using Cy2, Cy5 or Cy2-Cy5 settings, see Figure 3B. B. Calculated FRET efficiencies. F_D : Fluorescence intensity donor (lane 2, 4, 6 in Cy2 channel); F_{DA} : FRET intensity donor in presence of acceptor (lane 7-12 in Cy2 channel).

This result confirms the occurrence of intra-proteasomal FRET and the suitability of ABPs **1-6** for native-PAGE FRET analysis of proteasome compositions. Remarkably, mutual differences in fluorescence intensity on native-PAGE between samples treated with a single ABP was observed, while on SDS-PAGE the intensities are similar (Figure 5A, compare lanes 1-6 in both gels). For instance, BODIPY(FL)-NC001 **2** shows the highest fluorescent signal with the intensities for BODIPY(FL)-LU112 **4** and BODIPY(FL)-LU015 being respectively 1.5 and 4 times lower (Figure 5A, compare lane 2, 4 and 6). However, after gel fixation after which all FRET signals were lost, the fluorescence intensity for the three probes became almost equal. These differences may be caused by either self-quenching³⁵ or homo-FRET³⁶, processes that can take place when fluorophores have sufficient overlap in their excitation and emission spectra. Since proteasomes encompass two copies of each subunit (pair), two fluorophores are brought in close proximity, which allows self-quenching or homo-FRET processes to occur. Due to differences in the mutual orientation of- and distances between the two fluorophores, the efficiency of self-quenching of the ABPs may vary, resulting in different fluorescence intensities.

Native-PAGE FRET allows the detection of mixed proteasomes

In order to detect mixed proteasomes by native-PAGE FRET, each donor or acceptor ABP should bind to a single cCP or iCP subunit. The presence of mixed proteasome core particles in a given sample is revealed by FRET when, for instance, a donor ABP is bound to a cCP subunit and an acceptor ABP to an iCP subunit. Selective binding of ABPs **1-6** to a single subunit can be attained by making use of the panel of subunit-selective inhibitors which are described in chapter 3 (see also Table 2). With the exception of LU-002c (targeting β 2c) the selectivity windows for all inhibitors are sufficiently large to allow selective and complete blocking of their target subunits. With the panel of five inhibitors selective for β 1c, β 1i, β 2i, β 5c, or β 5i, eight combinations of two inhibitors can be made. With these and together with ABPs **1-6** eight different proteasome subunit combinations can in theory be detected. Each possible inhibitor combination was assessed in Raji cell lysates using two FRET ABP pairs (see Figure 6). Since both inter- and intra- β -ring FRET can take place, the observed FRET signal is a sum of several possible FRET pathways that emerge from, either, two, three or four ABPs present in a proteasome particle. This complexity essentially precludes the use of relative FRET intensity as a measurement for relative amounts of specific subunit combinations. Interestingly, however, clear FRET signals were observed for each combination, which implies that, next to cCP, iCP and m_s CP particles also m_a CP particles are present. The various ABP couples yield FRET signals of similar intensities, but subtle differences are observed (see Table 3). The FRET intensities derived from either cCP-cCP or iCP-iCP ABP pairs are always higher than those obtained from cCP-iCP probe/inhibitor combinations, a result that

supports the reported preferential formation of pure iCPs and cCPs over mCPs. The high $\beta 2c$ over $\beta 2i$ ratio (see Table 3) is reflected in the relatively high FRET intensities emerging from ABPs bound to $\beta 2c$ - $\beta 1c/\beta 5c$ compared to $\beta 2c$ - $\beta 1i/\beta 5i$, underscoring that $\beta 2c$ is preferentially incorporated together with $\beta 1c$ and $\beta 5c$ (as in cCP and $m_aCP_{1,2 \text{ or } 3}$, see Table 1). The low FRET signal between $\beta 2c$ - $\beta 1i$ (as in m_sCP_2 and $m_aCP_{2,5,8,9}$) reflects the preferential incorporation of $\beta 2i$ together with $\beta 1i$ (as in iCP and $m_aCP_{4,7,9,10}$).

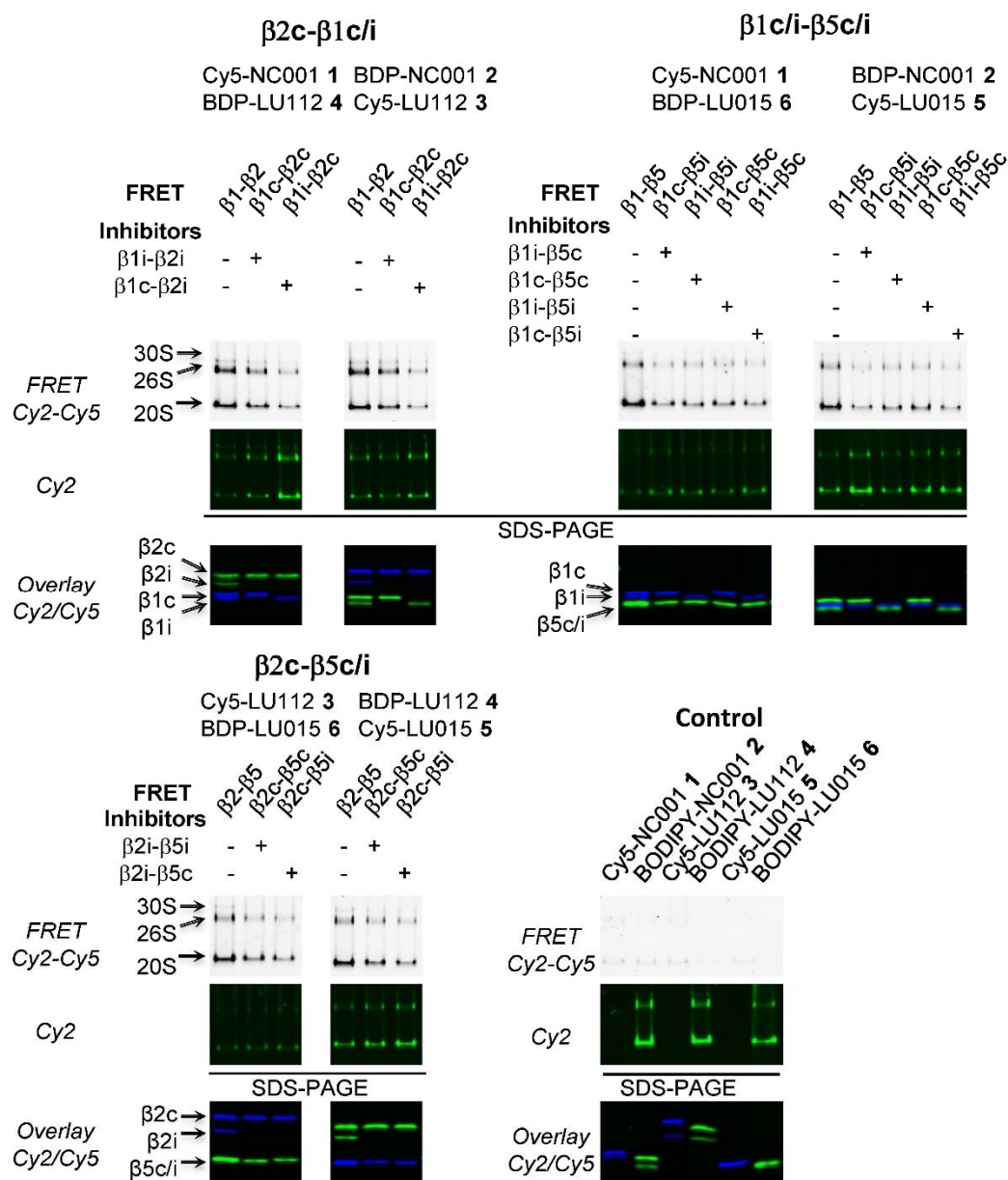


Figure 6. Detection of mixed proteasomes in Raji cell lysates. Samples were pre-incubated with indicated inhibitors, followed by labelling of residual proteasome activity by indicated ABPs. The samples were analysed by native-PAGE and SDS-PAGE.

Subunits		Relative FRET intensity (% of FRET no inhibitor)*		Ratio subunits**
ABPs		Cy5-NC001 – BDP-LU112 (1-4)	BDP-NC001 – Cy5-LU112 (2-3)	
β 1c	β 2c	53	50	β 1c/ β 1i= 1.24±0.03 (55/45)
β 1i	β 2c	18	17	β 2c/ β 2i= 2.28±0.07 (70/30)
ABPs		Cy5-NC001 – BDP-LU015 (1-6)	BDP-NC001 – Cy5-LU015 (2-5)	β 5c/ β 5i= 1.04±0.03 (51/49)
β 1c	β 5i	26	23	
β 1i	β 5i	28	35	
β 1c	β 5c	31	44	
β 1i	β 5c	23	20	
ABPs		Cy5-LU112 – BDP-LU015 (3-6)	BDP-LU112 – Cy5-LU015 (3-5)	
β 2c	β 5c	39	50	
β 2c	β 5i	27	29	

Table 3. Relative FRET intensities in Raji lysates. *Determined by quantification of FRET signals from Figure 6. ** Determined by quantification of SDS-PAGEs from Figure 6.

The FRET intensities for β 1c- β 5c and β 1i- β 5i are higher than those for β 1i- β 5c and β 1c- β 5i, indicating preferential formation of β 1c- β 5c and β 1i- β 5i containing β -rings. Remarkably, a substantial FRET signal was observed for β 1i- β 5c. As β 5i is required for the propeptide removal of β 1i, β 5c cannot be incorporated in the same β -ring together with β 5i, and therefore this result strongly suggests that m_aCP_2 and/or m_aCP_4 are present.

Asymmetric mixed proteasomes (m_aCPs) can be detected using native-PAGE FRET

When applied at appropriate concentrations, ABPs **7**, **8**, **9** and **10** selectively and completely block a single proteasome subunit, namely β 1c, β 1i, β 5c and β 5i respectively. Inclusion of these compounds in the native-PAGE FRET experiments allows labelling of for instance β 1c with a FRET donor and β 1i with a FRET acceptor ABP. FRET signals emerging from samples treated in this way and resolved on native-PAGE, can only be caused by m_aCPs . Clear FRET signals were observed for both FRET pairs **7/8** and **9/10**, confirming the presence of one or more m_aCPs (m_aCP_{1-4} : asymmetric in β 5 composition; $m_aCP_{2,4,5,7,8,10}$: asymmetric in β 1 composition) in Raji cell lysates (see Figure 7). Although relative amounts of m_aCPs could not be established due to lack of appropriate reference samples, this method demonstrates the presence of m_aCPs in a given sample in an unambiguous fashion.

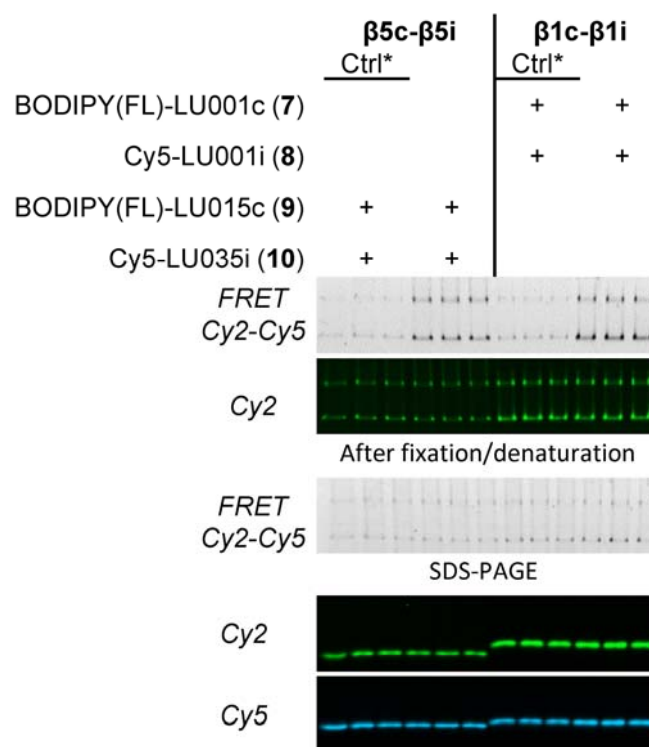


Figure 7. Asymmetric mixed proteasomes in Raji cell lysates. Samples were incubated with a $\beta 2$ -selective inhibitor (LU102, in case of ABPs 9, 10) or a $\beta 5$ -selective inhibitor (NC005, in case of ABPs 7, 7) followed by treatment with various ABPs. *Ctrl: control. Control samples contained twice the amount of protein compared to normal samples and were incubated with LU-102 or NC-005 as for normal samples, followed by incubation with one of the ABPs. Next, remaining proteasome activities were blocked by a mixture of NC001, LU102 and NC005 and the samples treated with ABP 7/8 and 9/10 were mixed. This shows the total background caused by the intrinsic properties of the fluorophores.

Assessment of proteasome composition after induction of iCPs by IFN- γ .

The expression of iCP subunits can be induced by exposure to the inflammatory cytokine interferon- γ (IFN- γ). Dahlmann and co-workers²¹ reported that HeLa cells exposed to IFN- γ express both m_s CPs and m_a CPs. These observations were re-evaluated using the above-described native-PAGE FRET assay. For this, HeLa cells were either exposed to IFN- γ for 24 h or left untreated. Next, both samples were subjected to various inhibitor/ABP combinations and evaluated by native-PAGE FRET as described above. When not exposed to IFN- γ , HeLa cells express only small amounts of $\beta 1i$ and $\beta 5i$ while $\beta 2i$ could not be detected. Following exposure to IFN- γ , a substantial increase of the amount of all iCP subunits was found (Table 4, Figure 8). As expected, non-exposed HeLa cells show high inter-cCP subunit FRET signals. Since the FRET signals emerging from $\beta 5i\text{-}\beta 1c$ are higher than those observed for $\beta 5i\text{-}\beta 1i$, it is likely that the majority of the $\beta 5i$ subunits in these non-exposed cells are present in proteasomes that also contain at least one $\beta 1c$ subunit (as in m_a CP_{1,2,5} and m_s CP₁). As well, substantial $\beta 5i\text{-}\beta 5c$ and $\beta 1i\text{-}\beta 1c$ FRET signals were observed (Figure 9), indicating the

presence of m_aCPs ($m_aCP_{1,2}$: asymmetric in $\beta 5$ composition; $m_aCP_{2,5}$: asymmetric in $\beta 1$ composition). Most likely, the majority of these m_aCPs contain either a single $\beta 5i$ (m_aCP_1), or both one $\beta 5i$ and one $\beta 1i$ in the same β -ring (m_aCP_2), as witnessed by the observed FRET signal between $\beta 5c$ and $\beta 1i$. After exposure to IFN- γ , a dramatic increase in $\beta 5i$ - $\beta 1i$ FRET signal is observed, while $\beta 5i$ - $\beta 1c$, $\beta 5c$ - $\beta 1i$ and $\beta 5c$ - $\beta 1c$ combinations are slightly decreased. This decrease does not necessarily reflect a decrease of the absolute amounts of these subunit-pairs, but is probably caused by the increase in expression and incorporation into proteasome particles of both $\beta 5i$ -subunits and $\beta 1i$ -subunits, with an increased total FRET intensity as the result.

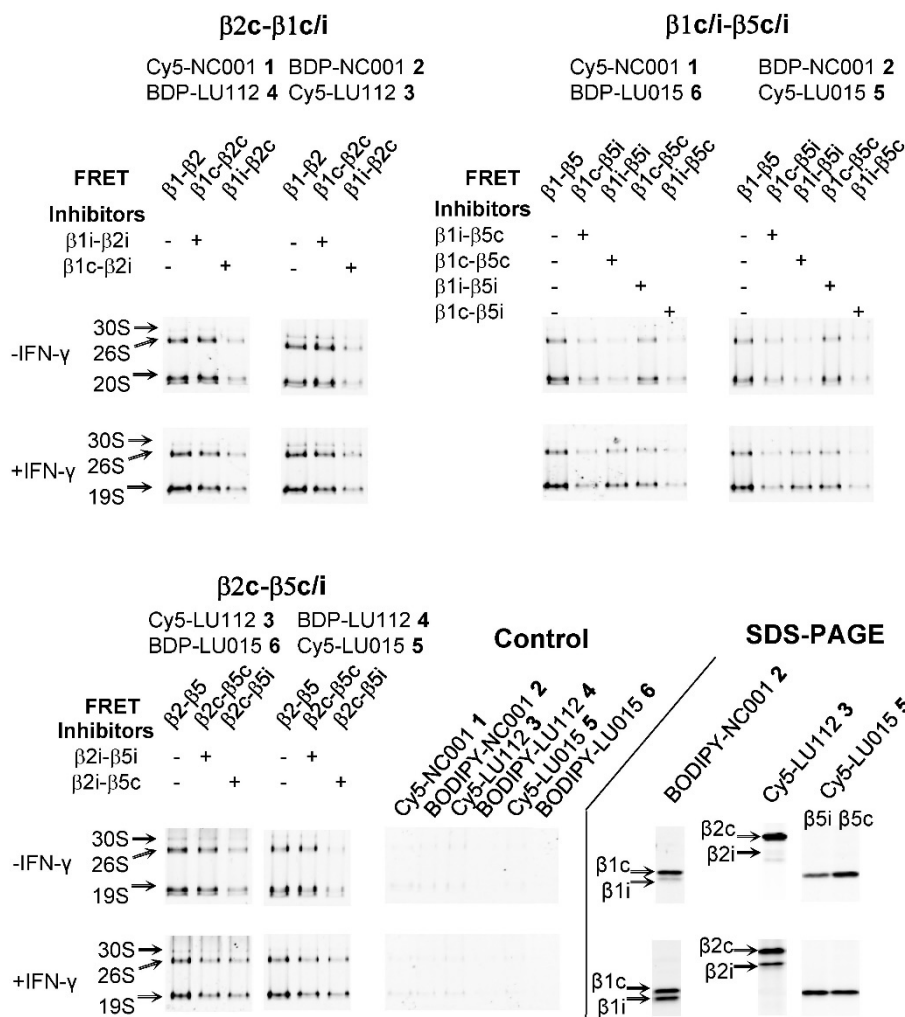


Figure 8. Mixed proteasomes in HeLa cell lysates, with or without exposure to IFN- γ for 24 h. Samples were pre-incubated with indicated inhibitors, followed by labelling of residual proteasome activity by indicated ABPs. SDS-PAGE analysis shows the relative amounts of iCP and cCP subunit before and after exposure to IFN- γ . To label $\beta 5c$ or $\beta 5i$ specifically, either $\beta 5i$ was blocked by LU-035i or $\beta 5c$ by LU-005c.

Subunits		Relative FRET intensity (% of FRET no inhibitor)*				Ratio subunits**
		-IFN- γ	+IFN- γ	-IFN- γ	+IFN- γ	
ABPs		Cy5-NC001-BDP-LU112 (1-4)		BDP-NC001-Cy5-LU112 (2-3)		-IFN- γ
β 1c	β 2c	89	57	102	58	β 1c/ β 1i= 5.52 \pm 0.04 (85/15)
β 1i	β 2c	22	20	20	19	β 2c/ β 2i= 1.00 (100/0)
ABPs		Cy5-NC001-BDP-LU015 (1-6)		BDP-NC001-Cy5-LU015 (2-5)		β 5c/ β 5i= 2.47 \pm 0.12 (72/28)
β 1c	β 5i	29	21	32	22	+IFN- γ
β 1i	β 5i	14	41	13	40	β 1c/ β 1i= 1.44 \pm 0.07 (85/59)
β 1c	β 5c	54	33	67	40	β 2c/ β 2i= 2.72 \pm 0.01 (100/37)
β 1i	β 5c	17	7	15	10	β 5c/ β 5i= 0.98 \pm 0.04 (72/72)
ABPs		Cy5-LU112-BDP-LU015 (3-6)		BDP-LU112-Cy5-LU015 (3-5)		
β 2c	β 5c	72	36	74	47	
β 2c	β 5i	30	30	19	31	

Table 4. Relative FRET intensities in HeLa lysates, before and after exposure to IFN- γ for 24 h. *Determined by quantification of FRET signals from Figure 9. ** Determined by quantification of SDS-PAGES.

Given the long half-life of cCPs (up to 5 days)¹⁵, IFN- γ induced expression of iCP subunits presumably leads to a net increase of the total proteasome amount. When for convenience it is assumed that limited proteasome degradation takes place during the 24 h exposure with IFN- γ , the slight decrease in β 5i- β 1c and β 5c- β 1i-derived FRET signals indicates that no new proteasomes containing these subunit-pairs are formed, that newly expressed β 5i is mainly incorporated together with β 1i and that newly formed CPs are symmetric with respect to their β 1/ β 5 subunit composition. Interestingly, the β 2c- β 5i FRET signals significantly increase (Figure 8) and their intensities become closer to the β 2c- β 5c FRET signals. The same applies to β 1i- β 2c, indicating that β 5i is to some extent incorporated with β 2c, which is also reflected by the lower net increased amount of β 2i (+37%) compared to β 1i and β 5i (both +44%). Altogether it can be concluded that, following exposure to IFN- γ , HeLa cells predominantly produce two distinct proteasome types, namely mCPs featuring β -rings composed of either β 1i- β 2i- β 5i or β 1i- β 2c- β 5i (as in iCP, m_sCP₂ and m_aCP₉). This observation is further confirmed by the lower relative amount of m_aCPs found after exposure to IFN- γ (lower signal/noise ratio compared to no IFN- γ , Figure 9), indicating that the newly formed proteasomes are symmetric with respect to their β 1 and β 5 subunit composition.

Discussion

This chapter describes an in-depth analysis on the use of ABPs to determine the composition of large protein complexes using a native-PAGE FRET assay. Proteasome subunit-pair selective ABPs equipped with suitable FRET donor and acceptor fluorophores were selected, which target β 1c/ β 1i, β 2c/ β 2i or β 5c/ β 5i. Crude cell extracts were treated with combinations of these FRET donor/acceptor ABPs and resolved on native-PAGE, after which FRET signals were measured by fluorescent imaging of the gel.

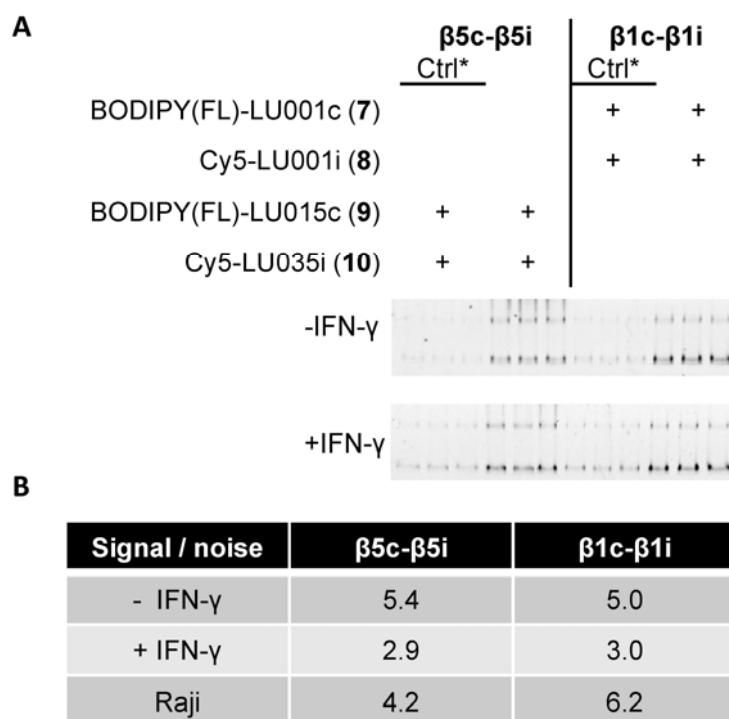


Figure 9. Asymmetric mixed proteasomes in HeLa cell lysates, before and after exposure to IFN- γ for 24 h. A. Samples were incubated with a $\beta 2$ -selective inhibitor (LU102, in case of ABPs **9**, **10**) or a $\beta 5$ -selective inhibitor (NC005, in case of ABPs **7**, **8**) followed by treatment with ABPs. *Ctrl: control. Control samples contained twice the amount of protein compared to normal samples and were incubated with LU-102 or NC-005 as for normal samples, followed by incubation with one of the ABPs. Next, remaining proteasome activity was blocked by a mixture of NC001, LU102 and NC005 and the samples treated with ABP **7/8** and **9/10** were mixed. This shows the total background caused by the intrinsic properties of the fluorophores. B. Signal/noise ratios of m_a CP FRET signals of HeLa cell lysates, before and after exposure to IFN- γ for 24 h, compared to Raji cell lysates.

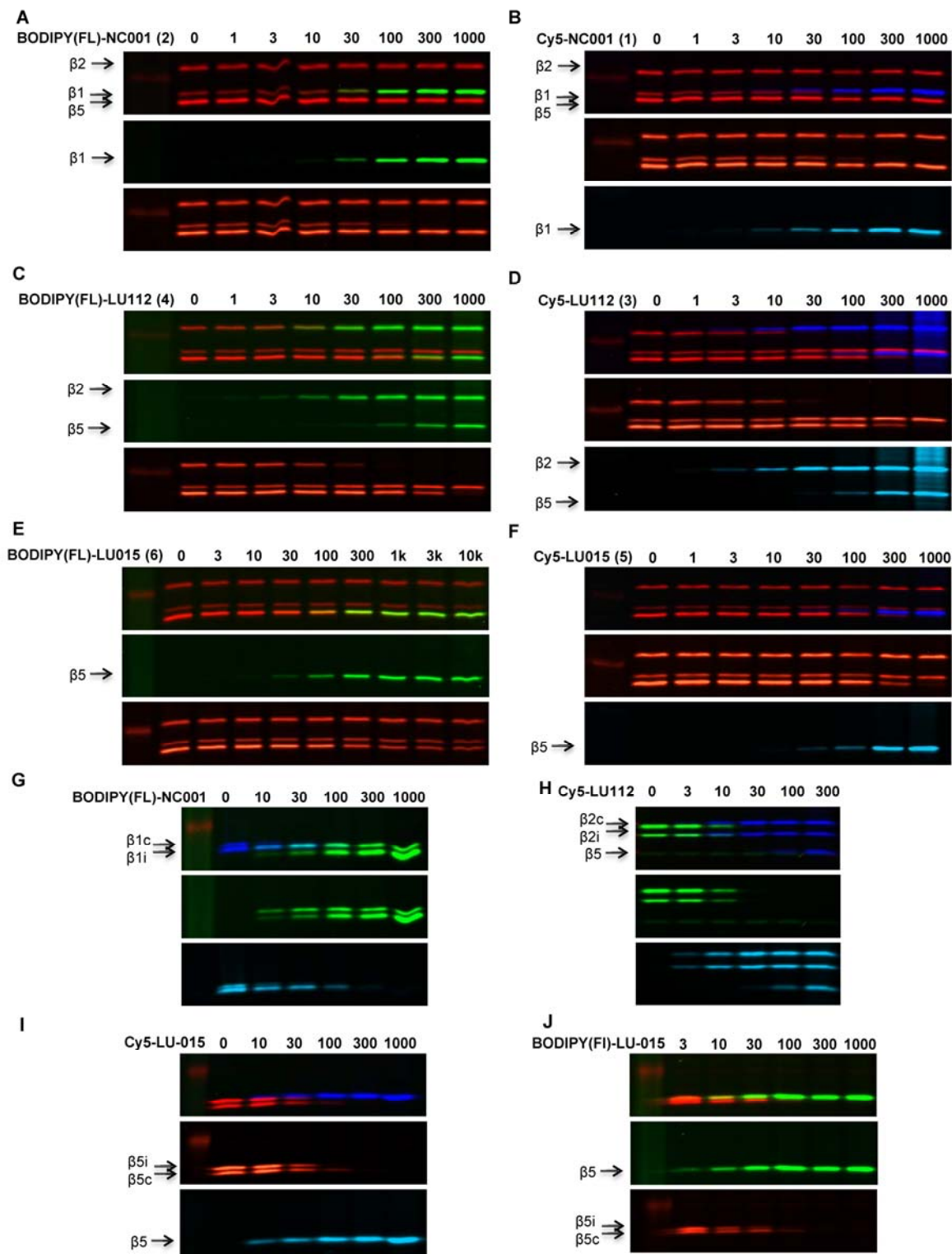
In HEK-293 cells, expressing exclusively cCPs, all FRET pairs gave clear FRET signals with high FRET efficiencies ($E > 0.8$), confirming that $\beta 1c$, $\beta 2c$ and $\beta 5c$ are present in stoichiometric amounts. The assembly pathway of immunoproteasomes favours the formation of CPs that contain only $\beta 1i$, $\beta 2i$ and $\beta 5i$, however, incorporation of both cCP and iCP subunits to form mCPs occurs as well, and in total 15 different 20S proteasomes can exist (see Table 1). Using subunit selective inhibitors, which block $\beta 1c$, $\beta 1i$, $\beta 2i$, $\beta 5c$ or $\beta 5i$, specific FRET signals derived from eight subunit-pairs were obtained. In lysates of Raji cells, which express all six proteasome subunits, FRET signals were observed for iCP-iCP and cCP-cCP subunit-pairs. Interestingly, also FRET signals of all possible iCP-cCP subunit-pairs could be detected, indicating the presence of mCPs. Moreover, using selective $\beta 1c-\beta 1i$ and $\beta 5c-\beta 5i$ targeting FRET donor-acceptor pairs, m_a CPs could be visualized that are asymmetric in their $\beta 1$ and $\beta 5$ subunits. Altogether, these results indicate a complex mixture of proteasome subtypes in Raji cells. Although this method does not provide the exact composition and neither absolute quantity of the different proteasome subtypes, relative FRET intensities do provide

semi-quantitative information regarding the presence of the different subunit-pairs. In Raji cells, iCP-iCP and cCP-cCP subunit-pairs show higher relative FRET intensities compared to iCP-cCP subunit-pairs for $\beta 1$ - $\beta 5$, indicating preferential formation of $\beta 1i$ - $\beta 5i$ and $\beta 1c$ - $\beta 5c$ containing β -rings. Compared to Raji cells, IFN- γ exposed HeLa cells do show much lower relative FRET intensities of $\beta 1$ - $\beta 5$ iCP-cCP subunit-pairs, and the relative FRET intensities indicate preferential formation of proteasomes containing β -rings composed of $\beta 5i$ - $\beta 1i$ - $\beta 2i$ and $\beta 5i$ - $\beta 1i$ - $\beta 2c$. Interestingly, both Raji- and IFN- γ exposed HeLa cells express similar amounts of all subunits, indicating that more mCPs are formed when all subunits are constitutively expressed compared to induction of iCP subunits in otherwise low iCP expressing cells. Remarkably, Dahlmann and co-workers identified CPs asymmetric in their $\beta 1$ subunit composition in IFN- γ exposed HeLa cells, while the non-exposed HeLa in their hands did not express detectable amount of immunoproteasome subunits.²¹ However, in this study it was found that after IFN- γ exposure HeLa cells predominantly express proteasome containing β -rings symmetric in their $\beta 1$ subunit composition. Dahlmann and co-workers used $\beta 1c$ -ZZ transfected HeLa cells to allow specific precipitation of $\beta 1$ -ZZ by binding to IgG and subsequent analysis of subunit composition of precipitated proteasomes. This might result in higher $\beta 1c$ -ZZ than normal $\beta 1c$ expression, causing higher incorporation of $\beta 1c$ -ZZ in newly formed proteasomes resulting in asymmetric proteasome formation.

Compared to existing methods to determine proteasome composition, the method described in this chapter has several advantages. For instance, van den Eynde and co-workers²² used subunit depletion and subsequent immunoblotting to determine proteasome composition. Alternatively, they calculated the quantity of mCPs based on the assumption that $\beta 5i$ can be incorporated as the only iCP subunit or together with $\beta 1i$, but that $\beta 2i$ is always incorporated together with $\beta 1i$ and $\beta 5i$. However, in these approaches asymmetric proteasomes are not taken into account and therefore several proteasome subtypes are possibly overlooked. This FRET-based approach, besides being more sensitive, is also much faster, straightforward and less time consuming than the methods relying on chromatographic separation of proteasomes. The measurement of FRET signals in-native PAGE also represents a major improvement the methodology developed by Kim and co-workers.³⁰ In this method, FRET signals were measured in a plate reader, which required removal of unbound probes by filtration. Moreover, whereas detect $\beta 5c$ - $\beta 1i$ FRET signals were detected, the detection of other subunit-pairs was hampered by the lack of truly subunit selective probes and inhibitors. Importantly, their method to prove $\beta 5c$ - $\beta 1i$ containing proteasomes is highly questionable, since a $\beta 5i$ selective probe (LKSCy5³⁷) was claimed to selectively label $\beta 5c$ and a $\beta 1c$ / $\beta 1i$ targeting probe (UKPCy3) was used to selectively label $\beta 1i$ in RPMI-8226 cells and no selective inhibitors were applied to inhibit $\beta 5i$ and $\beta 1c$.

In conclusion, the native-PAGE FRET assay described in this chapter adds to existing methods that allow the assessment of proteasome core particle composition. The method provides semi-quantitative insights in the abundance of ten different proteasome subunit-pairs and can do so in any crude cell extract.

Supporting Figure



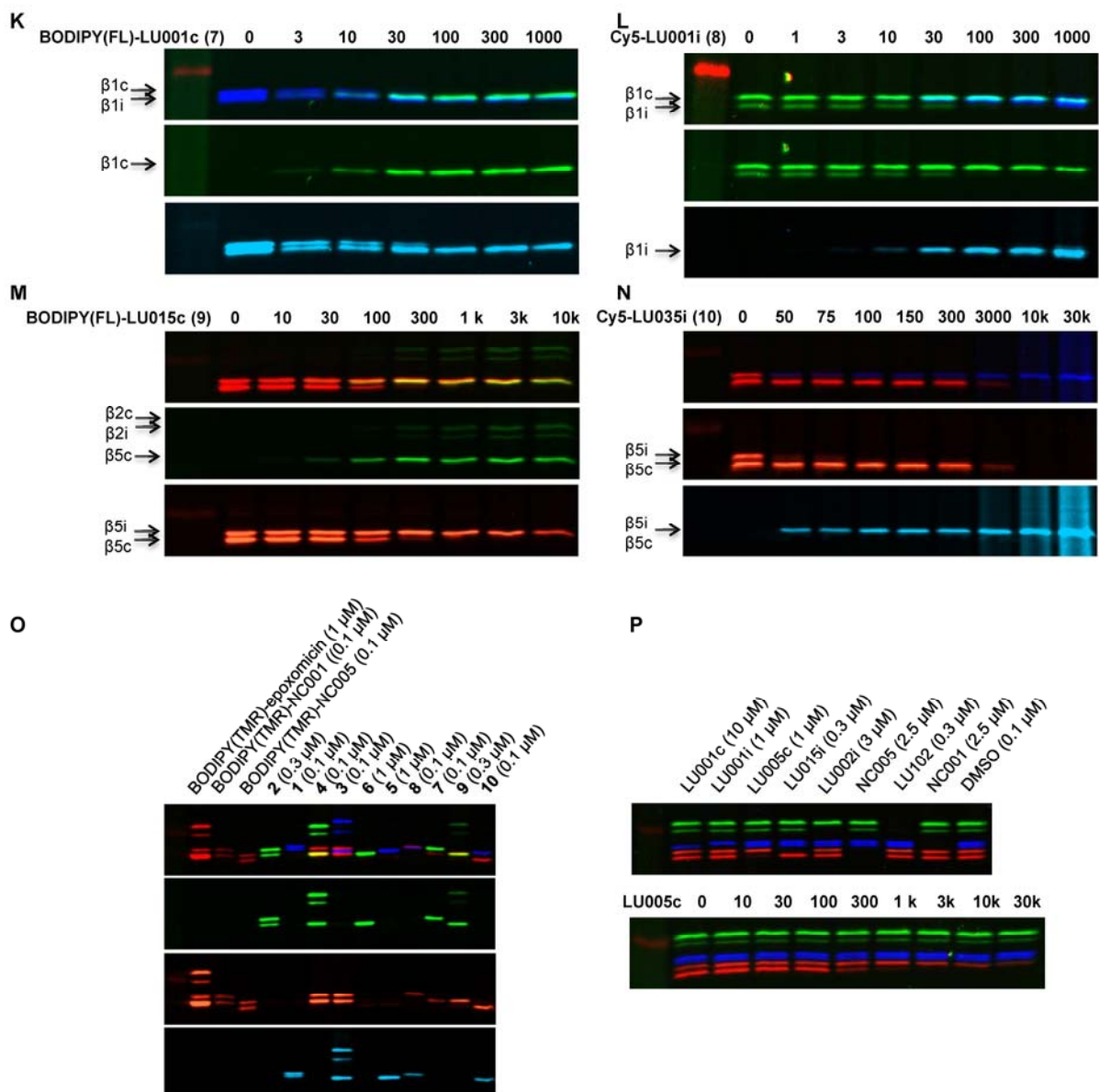


Figure S1. Labelling profiles of ABPs in HEK-293 (A-F) and Raji (G-N) to determine optimal probe concentrations, as indicated in Table 1 and verification of ABP labelling and selective inhibition by inhibitors in IFN- γ treated HeLa cells. For labelling profiles of Cy5-NC001 and BODIPY(FL)-LU112, see chapter 3. Upper gels picture is overlay of Cy2/Cy3, Cy3/Cy5 or Cy2/Cy5 channels. BODIPY(FL): depicted green; BODIPY(TMR): depicted red; Cy5: depicted blue. A-F. HEK-293 cell lysates were treated with indicated concentrations of ABP 1-6, followed by labelling of residual proteasome activity by labelling of residual $\beta 1$ activity by BODIPY(TMR)-epoxomicin (1 μM); G-N. Raji cell lysates were treated with indicated concentrations of ABPs followed by labelling of: residual $\beta 1$ activity by Cy5-NC001 (0.1 μM) (G, K) or BODIPY(FL)-NC001 (L); residual $\beta 2$ activity by BODIPY(FL)-LU112 (0.03 μM) (H); residual $\beta 5$ activity by BODIPY(TMR)-NC005 (0.1 μM) (I,J,M,N). O. Labelling of HeLa cell lysates by ABPs 1-10 at indicated concentrations followed by labelling of residual $\beta 1$ activity by BODIPY(TMR)-NC001 (0.1 μM) in case of $\beta 1$ selective ABPs; residual $\beta 2$ activity by BODIPY(TMR)-epoxomicin (1 μM) in case of $\beta 2$ selective ABPs and $\beta 5$ activity by BODIPY(TMR)-NC005 (0.1 μM) in case of $\beta 1$ selective ABPs. P. Verification of selective inhibition by inhibitors in IFN- γ treated HeLa cells.

Experimental

Synthetic procedures

General procedures

Acetonitrile (ACN), dichloromethane (DCM), N,N-dimethylformamide (DMF), methanol (MeOH), diisopropylethylamine (DiPEA) and trifluoroacetic acid (TFA) were of peptide synthesis grade, purchased at Biosolve, and used as received. All general chemicals (Fluka, Acros, Merck, Aldrich, Sigma, Iris Biotech) were used as received. Column chromatography was performed on Screening Devices b.v. Silica Gel, with a particle size of 40–63 μm and pore diameter of 60 \AA . TLC analysis was conducted on Merck aluminium sheets (Silica gel 60 F254). Compounds were visualized by UV absorption (254 nm), by spraying with a solution of $(\text{NH}_4)_6\text{Mo}_7\text{O}_{24}\cdot 4\text{H}_2\text{O}$ (25 g/L) and $(\text{NH}_4)_4\text{Ce}(\text{SO}_4)_4\cdot 2\text{H}_2\text{O}$ (10 g/L) in 10% sulphuric acid, a solution of KMnO_4 (20 g/L) and K_2CO_3 (10 g/L) in water, or ninhydrin (0.75 g/L) and acetic acid (12.5 mL/L) in ethanol, where appropriate, followed by charring at ca. 150 $^\circ\text{C}$. ^1H and ^{13}C NMR spectra were recorded on an AV-600 (600 MHz) spectrometer. Chemical shifts are given in ppm (δ) relative to CD_3OD as internal standard. High resolution mass spectra were recorded by direct injection (2 μL of a 2 μM solution in water/acetonitrile 50/50 (v/v) and 0.1% formic acid) on a mass spectrometer (Thermo Finnigan LTQ Orbitrap) equipped with an electrospray ion source in positive mode (source voltage 3.5 kV, sheath gas flow 10, capillary temperature 250 $^\circ\text{C}$) with resolution $R = 60,000$ at m/z 400 (mass range $m/z = 150\text{--}2,000$) and dioctylphthalate ($m/z = 391.28428$) as a “lock mass”. The high resolution mass spectrometer was calibrated prior to measurements with a calibration mixture (Thermo Finnigan). LC-MS analysis was performed on a Finnigan Surveyor HPLC system with a Gemini C_{18} 50 \times 4.60 mm column (detection at 200–600 nm), coupled to a Finnigan LCQ Advantage Max mass spectrometer with ESI. The applied buffers were H_2O , ACN and 1.0% aq. TFA. Method: xx \rightarrow xx% MeCN, 13.0 min (0 \rightarrow 0.5 min: 10% MeCN; 0.5 \rightarrow 8.5 min: gradient time; 8.5 \rightarrow 10.5 min: 90% MeCN; 10.5 \rightarrow 13.0 min: 10% MeCN). HPLC purification was performed on a Gilson HPLC system coupled to a Phenomenex Gemini 5 μm 250 \times 10 mm column and a GX281 fraction collector. LU112(Boc)³⁴, ABPs **1**³⁸, **2**³³, **4**³⁴; **5**, **6**, **8**, **10** (chapter 6); **7** (chapter 8); **9** (chapter 7) were synthesized as reported before. Subunit selective inhibitors are described in chapter 3.

Cy5-LU112 (3)

To a degassed solution of LU-112(Boc) (7.2 mg, 7.8 μmol) and Cy5-alkyne (5.2 mg) in DMF (0.8 mL) under an argon atmosphere was added $\text{CuSO}_4\cdot 5\text{H}_2\text{O}$ (0.5 equiv., 3.9 μmol (100 μL from degassed stock solution of 39 $\mu\text{mol}/\text{mL}$) and NaAsc (0.75 equiv., 5.9 μmol (100 μL from degassed stock solution of 59 $\mu\text{mol}/\text{mL}$)). After stirring overnight, the reaction mixture was concentrated and purified by column chromatography (0–2–5% MeOH in DCM). The Boc-protected compound was then treated with 1:1 TFA/DCM for 15 min, followed by concentration and purification by HPLC (C_{18} , 30–50% MeCN, 0.1% TFA, 10 min gradient) provided the product as a blue powder after lyophilisation (2.03 mg, 1.4 μmol , 18%). ^1H NMR (600 MHz, MeOD) δ 8.24 (t, $J = 13.0$ Hz, 2H), 7.82 (s, 1H), 7.49 (d, $J = 7.3$ Hz, 2H), 7.45 – 7.37 (m, 4H), 7.35 (d, $J = 8.1$ Hz, 2H), 7.32 – 7.23 (m, 5H), 7.23 – 7.10 (m, 5H), 7.06 (d, $J = 6.8$ Hz, 2H), 6.79 (dd, $J = 15.2, 5.5$ Hz, 1H), 6.67 – 6.49 (m, 2H), 6.27 (dd, $J = 13.7, 7.7$ Hz, 2H), 5.50 (dd, $J = 10.1, 5.6$ Hz, 1H), 4.82 – 4.78 (m, 1H), 4.62 (dd, $J = 10.3, 4.6$ Hz, 1H), 4.58 (s, 2H), 4.40 – 4.32 (m, 2H), 4.30 (dd, $J = 9.8, 5.1$ Hz, 1H), 4.09 (t, $J = 7.5$ Hz, 2H), 4.05 (d, $J = 7.7$ Hz, 3H), 3.61 (s, 3H), 3.49 – 3.39 (m, 1H), 3.24 – 3.13 (m, 1H), 3.12 – 2.96 (m, 2H), 2.92 (s, 3H), 2.86 (dd, $J = 14.0, 10.3$ Hz, 1H), 2.24 (t, $J = 7.4$ Hz, 2H), 1.88 – 1.78 (m, 2H), 1.77 – 1.65 (m, 12H), 1.65 – 1.54 (m, 3H), 1.47 (dt, $J = 11.6, 6.7$ Hz, 3H), 1.37 – 1.23 (m, 2H), 0.93 (dd, $J = 31.8, 6.3$ Hz, 6H). ^{13}C NMR (151 MHz, MeOD) δ 175.78, 175.51, 174.55, 174.32, 172.98, 169.46, 155.59, 155.43, 146.51, 146.15, 144.21, 143.56, 142.62, 142.53, 139.60, 139.39, 136.85, 133.10, 132.83, 131.99, 131.32, 130.94, 130.25, 130.04, 129.97, 129.75, 129.63, 128.20, 126.56, 126.35, 126.20, 123.80, 123.43, 123.29, 111.97, 111.88, 104.45, 104.16, 65.97, 55.92, 53.78, 52.64, 50.52, 44.74, 44.06,

44.03, 42.78, 41.84, 40.14, 39.09, 38.39, 36.56, 35.53, 31.53, 28.18, 27.96, 27.78, 27.42, 26.50, 25.90, 23.41, 21.96. HRMS: calculated $C_{72}H_{90}N_{11}O_6S$ 1236.67908[M]⁺; found 1236.67920. LC-MS (linear gradient 10 → 90% MeCN/H₂O, 0.1% TFA, 13.0 min):R_t (min): 6.22 (ESI-MS (m/z): 1236.67 (M⁺)).

Biochemical experiments

General

Lysates of cells were prepared by treating cell pellets with 4 volumes of lysis buffer containing 50 mM Tris pH 7.5, 2 mM DTT, 5 mM MgCl₂, 10% glycerol, 2 mM ATP, and 0.05% digitonin for 60 min. Protein concentration was determined using Qubit[®] protein assay kit (ThermoFisher). All cell lysate labelling experiments were performed in assay buffer containing 50 mM Tris pH 7.5, 2 mM DTT, 5 mM MgCl₂, 10% glycerol, 2 mM ATP. Cell lysate labelling and competition experiments were performed at 37°C. Incubation times were always 1 hour. Prior to fractionation on 12.5% SDS-PAGE (TRIS/glycine), samples were boiled for 3 min in a reducing gel loading buffer. The 7.5x10 cm (L x W) gels were run for 15 min at 80V followed by 120 min at 130V. NativePAGE[™] Novex[™] 3-12% Bis-Tris Protein Gels, 1.0 mm, 15-well, NativePAGE[™] Running Buffer (20X) and NativePAGE[™] Sample Buffer (4X) were obtained from ThermoFisher. Native gels were run for 115 min at 150V. In-gel detection of (residual) proteasome activity was performed in the wet gel slabs directly on a ChemiDoc[™] MP System using Cy2 setting to detect BODIPY(FL), Cy3 settings to detect BODIPY(TMR) and Cy5 settings to detect Cy5. FRET signal were detected using manual settings as indicated in Figure 3B.

FRET experiments

Final concentrations of ABPs and inhibitors are indicated in Table 1.

FRET with probes 1-6: Cell lysates (40 µg/sample, 18 µL) were treated with inhibitors (1 µL of 20x stocks in DMSO, inhibitors were premixed in case of multiple inhibitors) or DMSO. Samples for β1-β2 FRET were treated with NC005. After 1 h incubation, β5 selective ABPs **5** or **6** were added to the appropriate samples (1 µL of 20x stocks in DMSO) and the samples were incubated for 1 h (2 h for HEK), followed by the addition of β1 selective ABPs **1**, **2**, **3**, and/or **4** (1 µL of 20x stocks in DMSO). After incubation for 1 h, 8 µL of each samples was transferred for SDS-PAGE analysis. Another 8 µL was transferred for native-PAGE analysis, to which was added 4 µL NativePAGE sample buffer. Gels were run as described in the general section.

FRET with probes 7-10 (asymmetric proteasomes): Cell lysates (20 µg/sample, 18 µL) were first treated with LU102 (to inhibit β2 in the samples for β5c-β5i FRET) or NC005 (to inhibit β5 in the samples for β1c-β1i FRET) for 1 h. Subsequently, either ABPs **7** and **8** or **9** and **10** were added (1 µL of 20x stocks in DMSO) and the samples were incubated for 1 h. For the control samples, two separate vials for each sample containing cell lysates (40 µg/sample, 18 µL) were first treated with LU102 (to inhibit β2 in the samples for β5c-β5i FRET) or NC005 (to inhibit β5 in the samples for β1c-β1i FRET) for 1 h. To the first vial, ABPs **7** or **9** were added and to the second vial ABPs **8** or **10**. After incubation for 1 h, NC005 (to samples containing ABPs **7** or **8**, to inhibit residual β5 activities) or NC001 (to samples containing ABPs **7** or **8**, to inhibit residual β1 activities) were added and after incubation for 1 h, the samples containing ABPs **7/8** and **9/10** were mixed. The control samples contain the same amount of proteasome subunits labelled by the ABPs, however, the probes are not bound to the same CPs, thereby providing total background FRET signal, caused by the individual ABPs. All samples were analysed by SDS-PAGE and native-PAGE as described above.

Immunoproteasome induction in HeLa cells

HeLa cells were cultured in DMEM media supplemented with 10% fetal calf serum, GlutaMAX[™], penicillin, streptomycin in a 5% CO₂ humidified incubator. 3x10⁶ cells were seeded in a 10 cm dish and the cells were left to attach for 6 h, followed by the addition of IFN-γ (100 u/mL). The cells were grown for 24 h, and harvest by trypsin treatment, and washed with PBS. Lysates were prepared as described in the general section.

References

1. Hershko, A. & Ciechanover, A. The ubiquitin system. *Annu. Rev. Biochem.* **67**, 425-79 (1998).
2. Kisselev, A.F., Akopian, T.N., Woo, K.M. & Goldberg, A.L. The sizes of peptides generated from protein by mammalian 26 and 20 S proteasomes: implications for understanding the degradative mechanism and antigen presentation. *J. Biol. Chem.* **274**, 3363-3371 (1999).
3. Ferrington, D.A. & Gregerson, D.S. Immunoproteasomes: structure, function, and antigen presentation. *Prog. Mol. Biol. Transl. Sci.* **109**, 75-112 (2012).
4. McCarthy, M.K. & Weinberg, J.B. The immunoproteasome and viral infection: a complex regulator of inflammation. *Front. Microbiol.* **6**, doi: 10.3389/fmicb.2015.00021 (2015).
5. Tanaka, K. & Kasahara, M. The MHC class I ligand-generating system: roles of immunoproteasomes and the interferon-gamma-inducible proteasome activator PA28. *Immunol. Rev.* **163**, 161-176 (1998).
6. Murata, S., Yashiroda, H. & Tanaka, K. Molecular mechanisms of proteasome assembly. *Nat. Rev. Mol. Cell. Biol.* **10**, 104-115 (2009).
7. Kunjappu, M.J. & Hochstrasser, M. Assembly of the 20S proteasome. *Biochim. Biophys. Acta* **1843**, 2-12 (2014).
8. Hirano, Y. et al. A heterodimeric complex that promotes the assembly of mammalian 20S proteasomes. *Nature* **437**, 1381-1385 (2005).
9. Kusmierczyk, A.R., Kunjappu, M.J., Funakoshi, M. & Hochstrasser, M. A multimeric assembly factor controls the formation of alternative 20S proteasomes. *Nat. Struct. Mol. Biol.* **15**, 237-244 (2008).
10. Witt, E. et al. Characterisation of the newly identified human Ump1 homologue POMP and analysis of LMP7(β 5i) incorporation into 20 S proteasomes. *J. Mol. Biol.* **301**, 1-9 (2000).
11. Hirano, Y. et al. Dissecting β -ring assembly pathway of the mammalian 20S proteasome. *EMBO J.* **27**, 2204-2213 (2008).
12. Li, X., Kusmierczyk, A.R., Wong, P., Emili, A. & Hochstrasser, M. β -Subunit appendages promote 20S proteasome assembly by overcoming an Ump1-dependent checkpoint. *EMBO J.* **26**, 2339-2349 (2007).
13. Chen, P. & Hochstrasser, M. Autocatalytic subunit processing couples active site formation in the 20S proteasome to completion of assembly. *Cell* **86**, 961-972 (1996).
14. Ramos, P.C., Höckendorff, J., Johnson, E.S., Varshavsky, A. & Dohmen, R.J. Ump1p is required for proper maturation of the 20S proteasome and becomes its substrate upon completion of the assembly. *Cell* **92**, 489-499 (1998).
15. Heink, S., Ludwig, D., Kloetzel, P.-M. & Krüger, E. IFN- γ -induced immune adaptation of the proteasome system is an accelerated and transient response. *Proc. Natl. Acad. Sci.* **102**, 9241-9246 (2005).
16. Nandi, D., Woodward, E., Ginsburg, D.B. & Monaco, J.J. Intermediates in the formation of mouse 20S proteasomes: implications for the assembly of precursor beta subunits. *EMBO J.* **16**, 5363-5375 (1997).
17. Griffin, T.A. et al. Immunoproteasome assembly: cooperative incorporation of interferon γ (IFN- γ)-inducible subunits. *J. Exp. Med.* **187**, 97-104 (1998).
18. De, M. et al. β 2 subunit propeptides influence cooperative proteasome assembly. *J. Biol. Chem.* **278**, 6153-6159 (2003).
19. Groettrup, M., Standera, S., Stohwasser, R. & Kloetzel, P.M. The subunits MECL-1 and LMP2 are mutually required for incorporation into the 20S proteasome. *Proc. Natl. Acad. Sci.* **94**, 8970-8975 (1997).
20. Dahlmann, B., Ruppert, T., Kuehn, L., Merforth, S. & Kloetzel, P.-M. Different proteasome subtypes in a single tissue exhibit different enzymatic properties. *J. Mol. Biol.* **303**, 643-653 (2000).
21. Klare, N., Seeger, M., Janek, K., Jungblut, P.R. & Dahlmann, B. Intermediate-type 20 S proteasomes in HeLa cells: "asymmetric" subunit composition, diversity and adaptation. *J. Mol. Biol.* **373**, 1-10 (2007).
22. Guillaume, B. et al. Two abundant proteasome subtypes that uniquely process some antigens presented by HLA class I molecules. *Proc. Natl. Acad. Sci.* **107**, 18599-18604 (2010).

23. Guillaume, B. et al. Analysis of the processing of seven human tumor antigens by intermediate proteasomes. *J. Immunol.* **189**, 3538-3547 (2012).
24. Zanker, D., Waithman, J., Yewdell, J.W. & Chen, W. Mixed proteasomes function to increase viral peptide diversity and broaden antiviral CD8(+) T cell responses. *J. Immunol.* **191**, 52-59 (2013).
25. Dahlmann, B., Ruppert, T., Kloetzel, P.M. & Kuehn, L. Subtypes of 20S proteasomes from skeletal muscle. *Biochimie* **83**, 295-299 (2001).
26. Drews, O. et al. Mammalian proteasome subpopulations with distinct molecular compositions and proteolytic activities. *Mol. Cell. Proteomics* **6**, 2021-2031 (2007).
27. Pelletier, S. et al. Quantifying cross-tissue diversity in proteasome complexes by mass spectrometry. *Molecular BioSystems* **6**, 1450-1453 (2010).
28. Chirio-Lebrun, M.-C. & Prats, M. Fluorescence resonance energy transfer (FRET): theory and experiments. *Biochem. Educ.* **26**, 320-323 (1998).
29. Piston, D.W. & Kremers, G.-J. Fluorescent protein FRET: the good, the bad and the ugly. *Trends Biochem. Sci.* **32**, 407-414.
30. Park, J.E. et al. A FRET-based approach for identification of proteasome catalytic subunit composition. *Mol. BioSyst.* **10**, 196-200 (2014).
31. Borissenko, L. & Groll, M. 20S Proteasome and its Inhibitors: crystallographic knowledge for drug development. *Chem. Rev.* **107**, 687-717 (2007).
32. Elsasser, S., Schmidt, M. & Finley, D. in *Methods Enzymol.* 353-363 (Academic Press, 2005).
33. Verdoes, M. et al. A panel of subunit-selective activity-based proteasome probes. *Org. Biomol. Chem.* **8**, 2719-2727 (2010).
34. Geurink, P.P. et al. Incorporation of non-natural amino acids improves cell permeability and potency of specific inhibitors of proteasome trypsin-like sites. *J. Med. Chem.* **56**, 1262-1275 (2013).
35. Meer, B.W.v.d., III, G.C. & Chen, S.-Y.S. Resonance energy transfer. Theory and data. *VCH Publishers, New York*, 5-33 (1994).
36. Bader, A.N. et al. Homo-FRET imaging as a tool to quantify protein and lipid clustering. *ChemPhysChem* **12**, 475-483 (2011).
37. Sharma, L.K. et al. Activity-based near-infrared fluorescent probe for LMP7: a chemical proteomics tool for the immunoproteasome in living cells. *ChemBioChem* **13**, 1899-1903 (2012).
38. de Bruin, G. et al. A set of activity-based probes to visualize human (immuno)proteasome activities. *Angew. Chem. Int. Ed.* **55**, 4199-4203 (2016).